

Direct evidence for the suppression of period doubling in the bouncing-ball model

Piotr Pierański*

Department of Physics, University of Calabria, I-87036 Arcavacata di Rende, Cosenza, Italy

(Received 29 June 1987)

Direct experimental evidence for the suppression of period doubling by near-resonant perturbations is presented. The phenomenon is analyzed with use of the dissipative standard map approximation. Experimental results are compared with their numerically simulated counterparts.

Due to its mechanical, laboratory-scale construction, the bouncing-ball model makes one of the simplest physical objects in which some of the spectacular phenomena which appear in the nonlinear dynamical systems on their period-doubling route to chaos can be directly observed.¹⁻³ The period-doubling cascade itself,⁴ the virtual Hopf phenomenon,⁵⁻⁷ and the noise-sensitive hysteresis loops⁸⁻¹¹ are a few examples.

Recently, the model has been exploited¹² to provide experimental evidence for another, somewhat counterintuitive phenomenon described by Bryant and Wiesenfeld.¹³ As argued by the latter authors, a periodic perturbation of a near-resonant frequency $\nu_p \approx \nu_0/2$ (where ν_0 is the frequency of the mode in question below its period-doubling point) should always suppress the onset of period doubling. Applying a digital data acquisition system, Wiesenfeld and Tuffillaro¹² analyzed the behavior of the bouncing ball in presence of the near-resonant perturbation (added to the signal driving the collision surface) and provided a quantitative evidence for the $\frac{2}{3}$ power law describing the dependence of the bifurcation shift on the amplitude of the perturbation (see Fig. 8 in Ref. 12). Though extensive, the Wiesenfeld-Tuffillaro report seems to lack a clear illustration of the suppression phenomenon itself. It is the aim of this paper to present a series of storage oscilloscope recordings which would fill in the gap providing at the same time an evidence for another prediction of the Bryant-Weisenfeld theory: "...decreasing detuning enhances the suppression of period doubling." Since our report is supplementary to the extensive Ref. 12 we omit all technical details concerning the construction of the apparatus; basically it was the same as that described in our earlier papers.⁷ The only essential detail change in some of the presented experiments was the ball itself. Aiming at increasing the dissipation, we replaced the ball with a light but stiff plastic rod fixed elastically at one end and left free to bounce with its other end on the surface of a lens attached to the loudspeaker's membrane. In all reported experiments we observed the first period-doubling point $A_1^{(1)}$ located on the bifurcation tree of the $M^{(1)}$ mode of the bouncing ball (rod). While in this mode, the ball moves in a 1:1 resonance with the collision surface.

The nonlinearity parameter, amplitude A of the surface vibration, was always swept down through the $A_1^{(1)}$ bifurcation point. This choice results from our recent

study,¹⁰ where we demonstrated that bifurcation diagrams recorded at the up sweeps of the nonlinearity parameter display extreme sensitivity to noise which leads to a considerable scatter of their shape. The sweep-down versions of the bifurcation diagram do not display this instability.

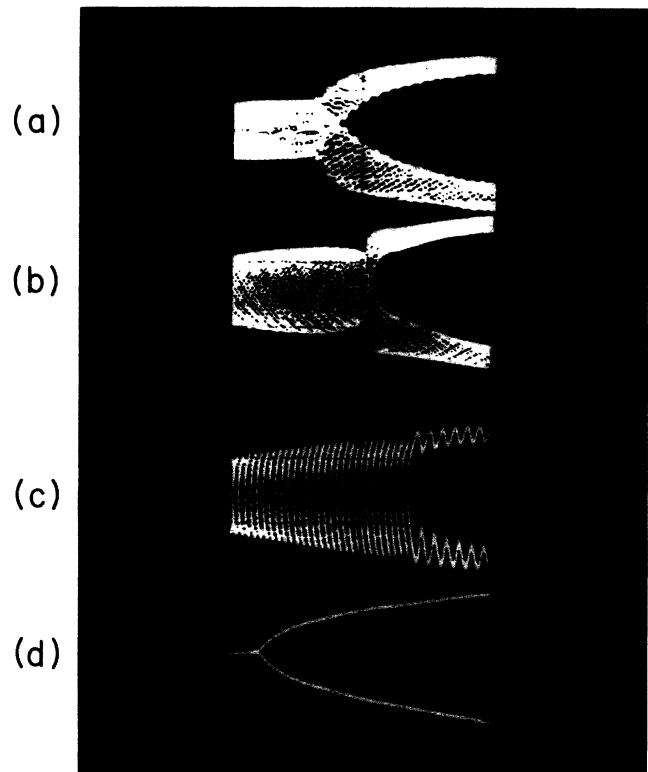


FIG. 1. Suppression of period doubling by near-resonant perturbations as observed within the bifurcation diagram of the $M^{(1)}$ mode of the bouncing-ball model (high dissipation case). Phases $\bar{\Theta}_i$ of collisions between the ball (rod) and the vibrating surface were plotted vs the amplitude of the ac signal driving the loudspeaker's membrane. The amplitude of the perturbation was the same for recordings (a), (b), and (c). Diagram (d) was recorded in the absence of the perturbation. The frequency ν_p/ν_0 was equal to 0.470, 0.482, and 0.495. The nonlinearity parameter, i.e., the amplitude of the surface vibration A , was swept down. $\nu_0=76$ Hz.

Fig. 1 presents a qualitative portrait of the suppression phenomenon. To make the shift of the bifurcation point well visible, we added to the three diagrams (a)–(c), recorded in the presence of near-resonant perturbations, the fourth one (d), obtained in absence of such a perturbation. Note that the bifurcation shift is largest within the diagram (c) obtained for the smallest detuning.

Aiming to obtain quantitative results concerning the dependence of the bifurcation shift on the detuning, we performed a series of experiments in which the frequency of the perturbation was changed in a regular manner (see Fig. 2). Looking at some of the recorded diagrams one may have some doubts whether the shifted bifurcation should be located at the point where the period-doubled branches start to protrude from the trunk of the $M^{(1)}$ mode, or at the point where they are seen really to separate. A close look at diagram (b), where ν_p/ν_0 was fixed close to the $\frac{4}{7}$ commensurability point, removes the

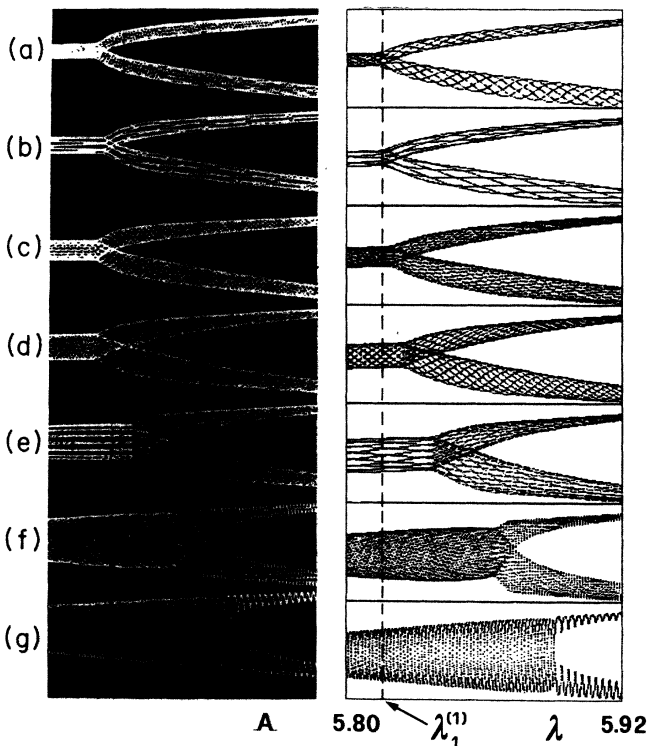


FIG. 2. Experimental (left) and numerical (right) bifurcation diagrams of the $M^{(1)}$ mode of the bouncing-ball model recorded in the presence of near-resonant perturbations (high dissipation case). In the experimental bifurcation diagrams the amplitude of the perturbation was the same in all experimental runs. The frequency ν_p/ν_0 was equal to 0.583, 0.568, 0.557, 0.543, 0.530, 0.517, and 0.508 for runs marked as (a)–(g), respectively. The nonlinearity parameter was swept down. $\nu_0=77$ Hz. In the numerical bifurcation diagrams the simulation was based on the dissipative standard map approximation, Eqs. (1), to which a periodic perturbation of frequency ν_p and amplitude ϵ was added. $\epsilon=0.015$ for all of the simulation runs while the frequency ν_p/ν_0 was equal to 0.584, 0.571 ($\cong \frac{4}{7}$), 0.559, 0.546, 0.533 ($\cong 8/15$), 0.521, and 0.508 for runs marked as (a)–(g), respectively. $k=0.15$.

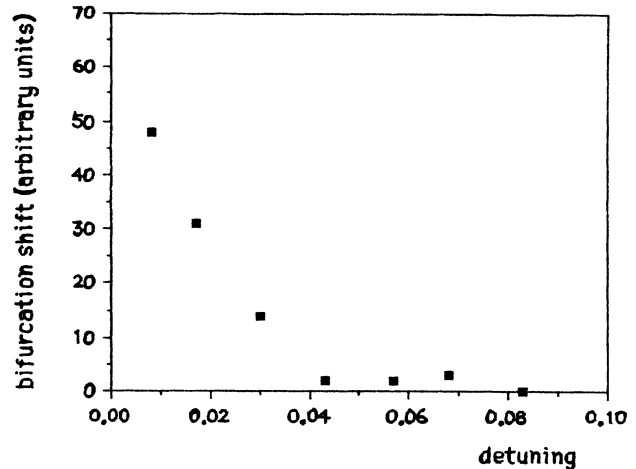


FIG. 3. Shift ΔA of the period-doubling bifurcation induced by periodic perturbation vs the detuning. Experimental data plotted in the figure were obtained from analysis of recordings shown in Fig. 2.

doubts. Obviously, the period-doubling symmetry breaking takes place at the former localization.

The shifts of the bifurcation point recorded in Fig. 2 were measured and plotted versus the detuning. Figure 3 presents the dependence. Clearly, the above-mentioned prediction of the Bryant-Wiesenfeld theory has been confirmed.

Recordings presented in Figs. 1 and 2 were obtained in experiments on the strongly dissipative bouncing rod version of the model. What happens when one changes the plastic rod for a highly elastic steel ball is shown in

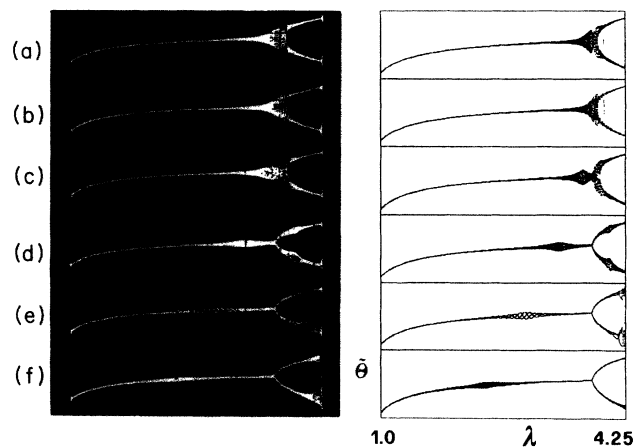


FIG. 4. Experimental (left) and numerical (right) bifurcation diagrams of the $M^{(1)}$ mode of the bouncing-ball model recorded in presence of near-resonant perturbations (low dissipation case). In the experimental bifurcation diagrams the amplitude of the periodic perturbation was the same for all of the recorded diagrams. The nonlinearity parameter was swept down. In the numerical bifurcation diagram simulation procedure was the same as for Fig. 2. $\epsilon=0.013$. The frequency ν_p/ν_0 was equal to 0.540, 0.488, 0.436, 0.384, 0.332, and 0.280 for runs marked (a)–(f), respectively. $k=0.85$.

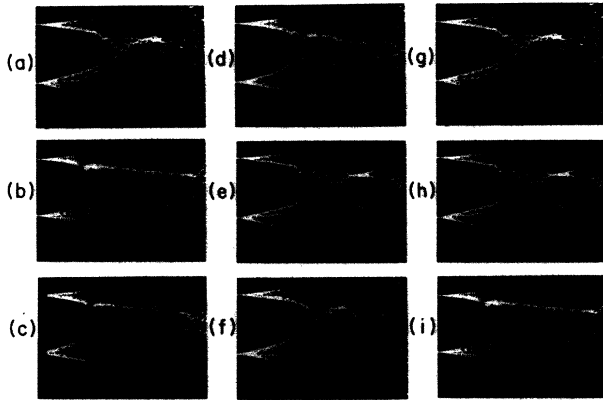


FIG. 5. Suppression of period doubling in the $M^{(1)}$ mode of the bouncing-ball model as seen in the experiments in which, at a fixed value of the nonlinearity parameter A^* , the amplitude of the periodic perturbation was swept linearly up (high dissipation case). The frequency ν_p/ν_0 was equal to 0.504, 0.491, 0.478, 0.465, 0.452, 0.439, 0.427, 0.418, and 0.405 for recordings (a)–(i), respectively. $\nu_0=77$ Hz. Note that in recordings (e)–(h) the increasing perturbation amplitude first suppresses the period doubling and squeezes the systems motion to a narrow region and then forces it to expand suddenly. In recording (i) the perturbation frequency was fixed close to the $\frac{2}{5}$ commensurability point.

Fig. 4. Weak damping makes the virtual Hopf phenomenon to appear, i.e., the response of the system to the periodic perturbation displays resonances located both below and above the period doubling point $A_1^{(1)}$. As long as the resonant peaks are located far from $A_1^{(1)}$, the bifurcation point remains practically intact. If, however, the peaks start to overlap at $\nu_p/\nu_0 \rightarrow \frac{1}{2}$, the diagram becomes significantly distorted and the bifurcation point shifts up.

Apart from the experimental diagrams Figs. 2 and 4 present their numerically simulated counterparts. The simulations were based on the dissipative standard map approximation of the ball's dynamics,

$$\nu_i = k\nu_{i-1} + \lambda \sin \tilde{\Theta}_i, \quad (1a)$$

$$\tilde{\Theta}_{i+1} = \tilde{\Theta}_i + \nu_i \pmod{2\pi}, \quad (1b)$$

where $\tilde{\Theta}_i$ denotes phases of the ball-surface collisions.

As seen from the figures, the approximation works very well. An extensive numerical study we performed indicates that in the vicinity of the period-doubling bifurcation point

$$\lambda_1^{(1)} = 2[(1+k)^2 + (1-k)^2 \Pi^2]^{1/2}, \quad (2)$$

the phase of every second collision, as calculated according to map (1), behaves like a point mass located in a potential well—single below the bifurcation point and dou-

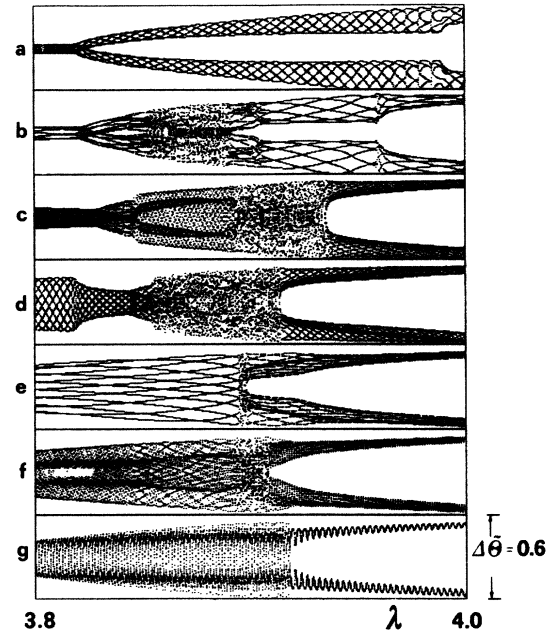


FIG. 6. Numerically simulated bifurcation diagrams of the $M^{(1)}$ mode of the bouncing ball in the presence of the near-resonant perturbation (low dissipation case). In diagrams (a)–(g) the perturbation frequency ν_p/ν_0 was equal to, respectively, 0.584, 0.571, 0.559, 0.546, 0.533, 0.521, and 0.508. Perturbation amplitude $\epsilon = 1.6 \times 10^{-2}$. $k = 0.85$.

ble above it. In this representation the near-resonant perturbation added to map (1) is seen as an external force oscillating at the beat frequency $\Delta\nu = \nu_p - \nu_0/2$. An effective viscosity present within the well depends on the restitution factor k ; see Eq. (1a). For $k \cong 1$ the model is nearly conservative and its motion, in presence of a slowly oscillating external force, may become very complex. In this case one observes strong departures from the simple scenario of the suppression phenomenon described in Ref. 12 (See Figs. 5 and 6). However, no matter what k , there is always such a neighborhood of the bifurcation point $(\lambda_1^{(1)}, \lambda_1^{(1)} + \delta)$, in which the frequencies of the local extrema of the effective potential well are so low that (at constant viscosity) the system becomes overdamped and the Bryant-Wiesenfeld description recovers its validity.¹⁴ Obviously, for small δ the barrier between the local minima of the double well is very low and the suppression phenomenon occurs at small amplitudes of the periodic perturbation.

This work has been done under Polish Academy of Sciences Project No. CPBP-01-12. The author thanks the staff of the Department of Physics, University of Calabria, in particular, R. Bartolino, for hospitality. Helpful correspondence from K. Wiesenfeld and N. Tuffillaro is gratefully acknowledged.

*Permanent address: Institute of Molecular Physics, Polish Academy of Sciences, Smoluchowskiego 17, PL-60-179 Poznań, Poland.

¹P. J. Holmes, *J. Sound. Vib.* **84**, 173 (1982).

²P. Pierański, *J. Phys. (Paris)* **44**, 573 (1983).

³N. B. Tuffillaro *et al.*, *J. Phys. (Paris)* **47**, 1477 (1986); S. Celaschi and R. L. Zimmerman, *Phys. Lett.* **120**, 447 (1987).

⁴For the list of references see, e.g., *Chaos*, edited by Hao Bai-

- Lin (World Scientific, Singapore, 1984).
- ⁵K. Wiesenfeld, *Phys. Rev. A* **32**, 1744 (1985).
- ⁶B. Derighetti, M. Ravani, R. Stoop, P. F. Meier, E. Brun, and R. Badii, *Phys. Rev. Lett.* **55**, 1746 (1985).
- ⁷P. Pierański and J. Małecki, *Phys. Rev. A* **34**, 582 (1986).
- ⁸R. Kapral and P. Mandel, *Phys. Rev. A* **32**, 1076 (1985).
- ⁹G. Broggi, A. Colombo, L. A. Lugiato, and P. Mandel, *Phys. Rev. A* **33**, 3635 (1986).
- ¹⁰P. Pierański and J. Malecki, *Nuovo Cimento* (to be published).
- ¹¹L. Fronzoni, F. Moss, and P. V. McClintock, *Phys. Rev. A* **36**, 1492 (1987).
- ¹²K. Wiesenfeld and N. B. Tufillaro, *Physica D (Utrecht)* **26**, 321 (1987).
- ¹³P. Bryant and K. Wiesenfeld, *Phys. Rev. A* **33**, 2525 (1986).
- ¹⁴We thank K. Wiesenfeld for drawing our attention to this essential conclusion.

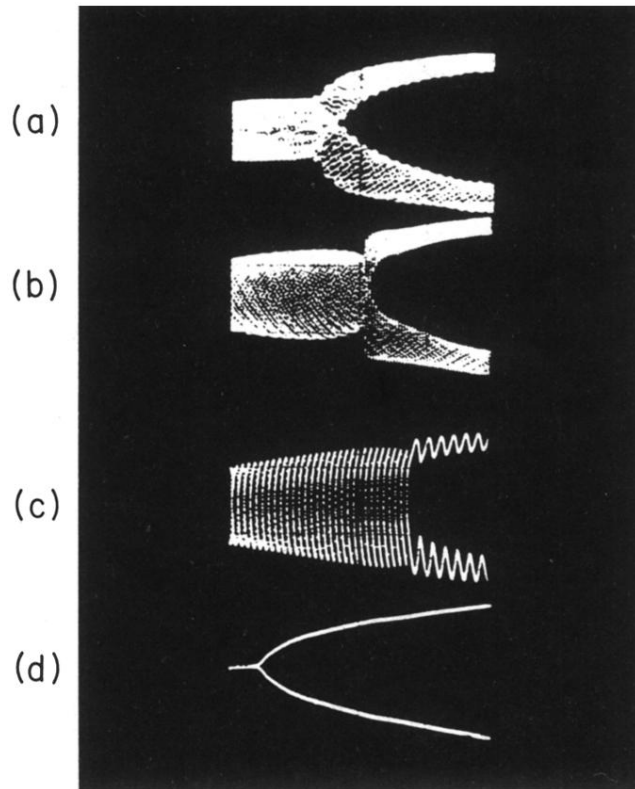


FIG. 1. Suppression of period doubling by near-resonant perturbations as observed within the bifurcation diagram of the $M^{(1)}$ mode of the bouncing-ball model (high dissipation case). Phases $\tilde{\Theta}_i$ of collisions between the ball (rod) and the vibrating surface were plotted vs the amplitude of the ac signal driving the loudspeaker's membrane. The amplitude of the perturbation was the same for recordings (a), (b), and (c). Diagram (d) was recorded in the absence of the perturbation. The frequency ν_p/ν_0 was equal to 0.470, 0.482, and 0.495. The nonlinearity parameter, i.e., the amplitude of the surface vibration A , was swept down. $\nu_0=76$ Hz.

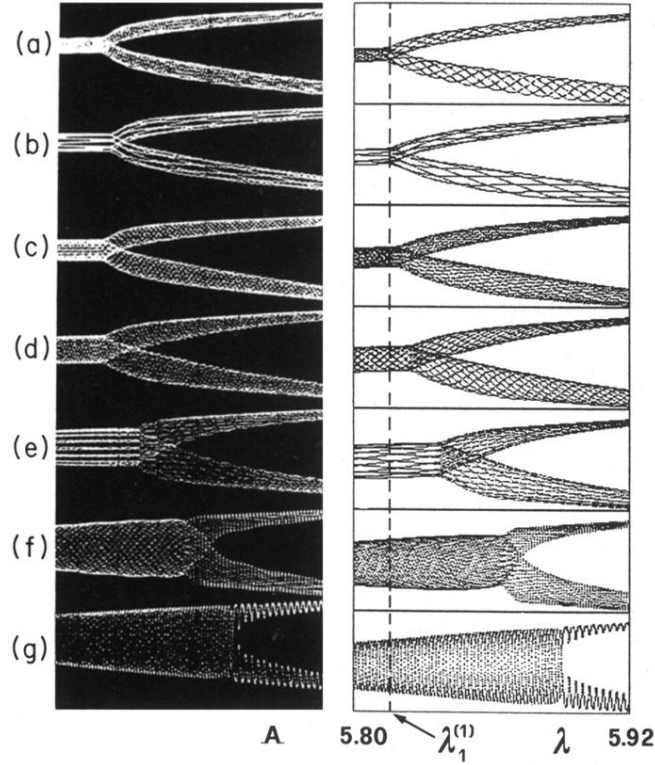


FIG. 2. Experimental (left) and numerical (right) bifurcation diagrams of the $M^{(1)}$ mode of the bouncing-ball model recorded in the presence of near-resonant perturbations (high dissipation case). In the experimental bifurcation diagrams the amplitude of the perturbation was the same in all experimental runs. The frequency ν_p/ν_0 was equal to 0.583, 0.568, 0.557, 0.543, 0.530, 0.517, and 0.508 for runs marked as (a)–(g), respectively. The nonlinearity parameter was swept down. $\nu_0=77$ Hz. In the numerical bifurcation diagrams the simulation was based on the dissipative standard map approximation, Eqs. (1), to which a periodic perturbation of frequency ν_p and amplitude ϵ was added. $\epsilon=0.015$ for all of the simulation runs while the frequency ν_p/ν_0 was equal to 0.584, 0.571 ($\cong \frac{4}{7}$), 0.559, 0.546, 0.533 ($\cong 8/15$), 0.521, and 0.508 for runs marked as (a)–(g), respectively. $k=0.15$.

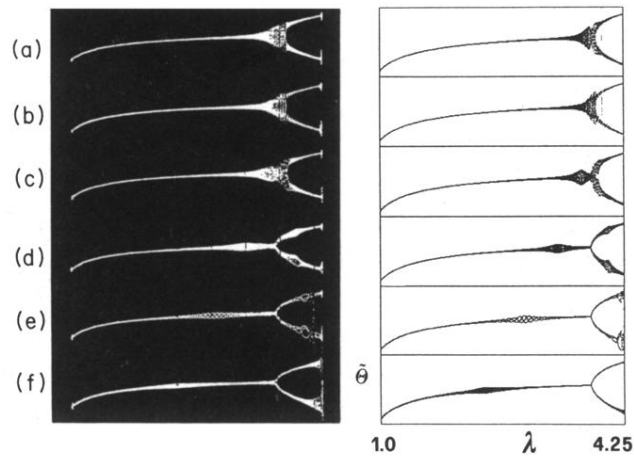


FIG. 4. Experimental (left) and numerical (right) bifurcation diagrams of the $M^{(1)}$ mode of the bouncing-ball model recorded in presence of near-resonant perturbations (low dissipation case). In the experimental bifurcation diagrams the amplitude of the periodic perturbation was the same for all of the recorded diagrams. The nonlinearity parameter was swept down. In the numerical bifurcation diagram simulation procedure was the same as for Fig. 2. $\epsilon=0.013$. The frequency ν_p/ν_0 was equal to 0.540, 0.488, 0.436, 0.384, 0.332, and 0.280 for runs marked (a)–(f), respectively. $k=0.85$.

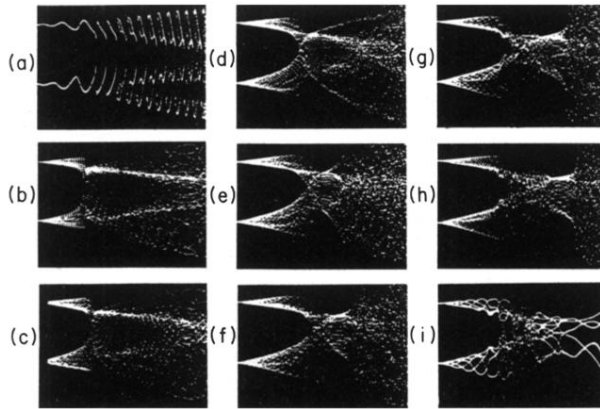


FIG. 5. Suppression of period doubling in the $M^{(1)}$ mode of the bouncing-ball model as seen in the experiments in which, at a fixed value of the nonlinearity parameter A^* , the amplitude of the periodic perturbation was swept linearly up (high dissipation case). The frequency ν_p/ν_0 was equal to 0.504, 0.491, 0.478, 0.465, 0.452, 0.439, 0.427, 0.418, and 0.405 for recordings (a)–(i), respectively. $\nu_0=77$ Hz. Note that in recordings (e)–(h) the increasing perturbation amplitude first suppresses the period doubling and squeezes the systems motion to a narrow region and then forces it to expand suddenly. In recording (i) the perturbation frequency was fixed close to the $\frac{2}{5}$ commensurability point.

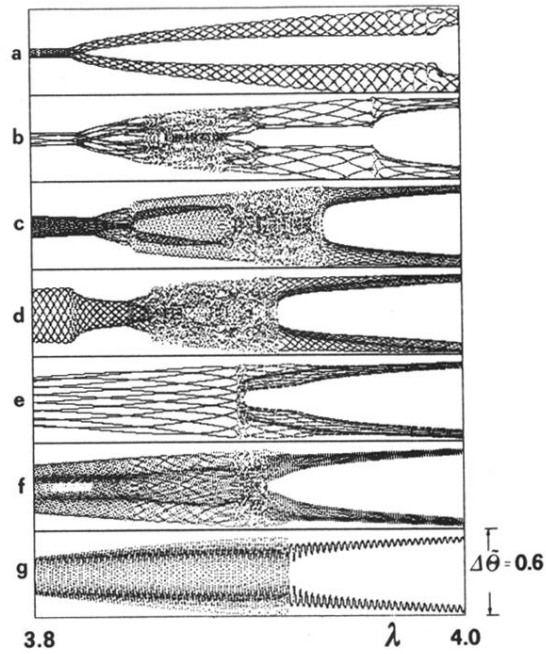


FIG. 6. Numerically simulated bifurcation diagrams of the $M^{(1)}$ mode of the bouncing ball in the presence of the near-resonant perturbation (low dissipation case). In diagrams (a)–(g) the perturbation frequency ν_p/ν_0 was equal to, respectively, 0.584, 0.571, 0.559, 0.546, 0.533, 0.521, and 0.508. Perturbation amplitude $\epsilon = 1.6 \times 10^{-2}$. $k = 0.85$.